Experimental evidence of the Frenkel line in supercritical neon

C. Prescher,[1] Yu. D. Fomin,[2] V. B. Prakapenka,[3] J. Stefanski,[1] K. Trachenko,[4] and V. V. Brazhkin[2]
[1]*Institut für Geologie und Mineralogie, Universität zu Köln, 50674 Köln, Germany*
[2]*Institute for High Pressure Physics, Russian Academy of Sciences, Troitsk 108840, Moscow, Russia*
[3]*Center for Advanced Radiation Sources, University of Chicago, Chicago, Illinois 60637, USA*
[4]*School of Physics and Astronomy, Queen Mary University of London, Mile End Road, London E1 4NS, United Kingdom*
(Received 5 August 2016; revised manuscript received 10 April 2017; published 26 April 2017)

Recent research suggests that the supercritical state consists of liquidlike and gaslike states where particle dynamics and key system properties are qualitatively different. We report experimental evidence of the structural crossover in supercritical neon at pressure and temperature conditions significantly exceeding the critical point values: 250 P_c and 6.6 T_c. The experimental results show a crossover of the medium-range order structure evidenced by the change of the structure factor with pressure. We also observe the crossover of the short-range order structure indicated by changes in the coordination number. The relative width of the crossover is fairly narrow and is smaller than 10–12% in pressure and temperature. By comparing our experimental results with molecular dynamics simulations, we suggest that the observed crossover can be attributed to the Frenkel line and discuss the relationship between the structural crossover and qualitative changes of dynamical and thermodynamic properties of supercritical matter.

DOI: 10.1103/PhysRevB.95.134114

I. INTRODUCTION

Supercritical fluids, the state of matter above the critical point, are considered uniform in terms of structure and properties. More recently, experiments have shown that the dynamic structure factor undergoes qualitative changes in the supercritical state [1–3]. To explain this, several mechanisms were proposed which involved analogues of the liquid-gas transitions in the supercritical state: the Fisher-Widom line demarcating different regimes of decay of structural correlations [4–6], several versions of percolation lines forming across conditional bonds or particles [7,8], or "thermodynamic" continuation of the boiling line such as the Widom line [9]. All these proposed mechanisms were later recognized to have issues which are not currently resolved. The Fisher-Widom line exists only in a stable fluid for model low-dimensional systems. The percolation lines are defined in realistic fluids only under specific conditions. The line of maxima of the correlation length (the Widom line) and other properties such as heat capacity, compressibility, or thermal expansion depend on the path in the phase diagram and do not extend far beyond the critical point [10–13].

In 2012, a new dynamic line in the supercritical region of the phase diagram was proposed, the Frenkel line [14–17]. Crossing the Frenkel line (FL) on temperature increase (pressure decrease) corresponds to the qualitative change of particle dynamics, from the combined oscillatory and diffusive motion as in liquids to purely diffusive motion as in gases. Simultaneously, high-frequency shear rigidity disappears (transverse excitations become depleted at all frequencies [18]), bringing the specific heat close to $c_v = 2k_B$ [17]. Other important changes take place at the liquidlike to gaslike crossover at the FL or close to it, including temperature and pressure dependencies of the sound speed, diffusion coefficient, viscosity, and thermal conductivity [16,17].

Practically, the FL can be located on the basis of presence or absence of oscillations in the velocity autocorrelation function, the criterion that coincides with $c_v = 2k_B$ [17]. The location of the FL has been calculated for several systems, including Ar, Fe, H_2O, CO_2, and CH_4 [16,17,19–21] where it was established that the temperature at the FL is about 3–5 times higher than the melting temperature at the same pressure. However, no experimental study of the Frenkel line was performed.

Importantly, the liquidlike to gaslike crossover at the FL should be accompanied by the *structural* crossover of the supercritical fluid. This follows from the dynamical crossover of particle motion and can also be inferred on the basis of the relationship between the structure and the thermodynamic crossover as discussed below in detail. Modeling data suggest the crossover of short-range order at the FL [22], yet no experimental evidence supports this prediction. Moreover, it is unclear whether the medium-range order, extensively studied in disordered systems, is sensitive to the FL.

Liquid structure was studied at pressures higher than the critical pressure but often at temperatures close to the melting line. Some of the previous work was aimed at elucidating the structure of supercritical water at a temperature higher than the melting temperature [23]. The structure of argon was studied at high temperature and pressure [24], albeit at conditions below the FL according to our calculations. As a result, no structural crossover was detected. Another study of argon [25] addressed the structure at supercritical conditions. Similarly to the previous work [24], the pressure and temperature were below the FL. Although sharp changes of structural parameters were discussed, these changes were not related to crossing the FL but coincided with, and were the result of, sharp changes in the chosen pressure-temperature path [26].

Experimental detection of the crossover at the FL in many interesting systems is challenging, because it requires the combination of high temperature and relatively low pressure. At these conditions, many types of standard high-pressure apparatus such as diamond anvil cells (DAC) cannot be used. We have therefore chosen neon with very low melting and critical temperature ($T_c = 44.5$ K) and fairly high critical pressure ($P_c = 2.68$ MPa). Room temperature is 6.6 times

higher than T_c, i.e., neon at room temperature and high pressure is a strongly overheated supercritical fluid. For the Lennard-Jones (LJ) fluid, the pressure corresponding to $6.6T_c$ at the FL is about $250P_c$, or 0.6−0.7 GPa for neon [17]. This pressure range is suitable for the DAC.

II. METHODS

The main aim of this study is an experimental detection of a possible structural crossover in supercritical neon at the FL. We employed symmetric DAC with a culet size of 300 μm. Re was used as gasket material and the cell was loaded with Ne at a GSECARS gas-loading system [27] to an initial pressure of 0.26 GPa. The pressure was fine controlled by a membrane system and estimated by the shift of the ruby fluorescence line [28]. The x-ray diffraction experiments were performed at the GSECARS, 13-IDD beamline, APS. An incident monochromatic x-ray beam with an energy of 45 keV and 2.5×3 μm spot size was used. In order to suppress the Compton scattering of the diamond anvils, a multichannel collimator (MCC) as described in Ref. [29] was employed. X-ray diffraction data was collected with a Mar345 image plate detector and the geometry was calibrated using LaB_6 standard. Collection time was 300 seconds. The background was measured with an empty cell prior to gas loading.

Detector calibration, image integration, and intensity corrections for oblique x-ray to detector angle, cBN seat absorption, and diamond absorption were performed using Dioptas software package [30]. The resulting diffraction patterns were corrected for an additional diamond Compton scattering contribution, which was necessary because the background measurement prior to compression was measured with a thicker sample chamber than the compressed sample at high pressure. The smaller sample chamber results in more diamond in the volume of diffraction constrained by the MCC. Both the sample signal and the additional diamond Compton scattering contribution were corrected with an MCC transfer function [29].

Structure factors and pair distribution functions were calculated following the procedure described in Ref. [31]. We employed the amount of diamond Compton scattering contribution in addition to the density and background scaling as an additional optimization variable. A Lorch modification function was employed during the Fourier transform in order to minimize unphysical oscillations due to cutoff effects. Structure factors were obtained up to $k_{max} = 7.5$ Å^{-1}.

The experimental study is supported and complemented by molecular dynamics (MD) simulations. We have used the LJ potential with parameters $\sigma = 2.775$ Å and $\varepsilon = 36.831$ K [32] and simulated 4000 particles in a cubic box with periodic boundary conditions. The equilibration was first performed in the canonical ensemble at each state point, followed by the production run in the microcanonical ensemble with 0.2 fs timestep for 2×10^6 steps. We find that averaging of calculated properties (such as the speed of sound) over this large number of timesteps is required to reduce the noise and errors.

We have simulated 15 pressure points in the range 0.05–3.7 GPa, corresponding to the density range of 0.3–2.2 g/cm^3. We have used the LAMMPS MD simulation package [33]. The structure factors $S(k)$ were calculated in MD simulations as Fourier transforms of the pair distribution functions $g(r)$:

$$S(k) = 1 + 4\pi\frac{N}{V}\int_0^\infty (g(r)-1)\frac{r\sin(kr)}{k}dr, \qquad (1)$$

where N/V is the number density of fluid.

III. RESULTS AND DISCUSSION

Experimental and simulated structure factors $S(k)$ and their corresponding pair distribution functions $g(r)$ are shown in Fig. 1. We observe very good agreement between experimental results and MD simulations. The position and height of the first peak of $S(k)$ (Fig. 2) show a change of slope against pressure at around 0.65 GPa. We further plot the height of the first three peaks of $g(r)$ vs pressure in Figs. 3(a)–3(c). While the maxima of the first two peaks show only slight changes of slope with pressure, the maximum of the third peak indicates two regimes: a constant value up to 0.65 GPa and a linear increase above. However, the constant height below 0.65 GPa is only within the error bars [Figs. 1(c) and 3(c)]. Thus, the plateau could be caused by the lack of data accuracy to detect a further decrease in the peak height. Nevertheless, the data in Fig. 3(c) show a crossover at 0.65 GPa.

Coordination number (CN) of neon against pressure is shown in Fig. 3(d). CN was obtained by integration over the first peak of $g(r)$ up to the first minimum r_{min} after the peak using:

$$CN = 4\pi\rho\int_0^{r_{min}} r^2 g(r)dr, \qquad (2)$$

where $\rho = N/V$ is number density. We observe a strong increase in CN from 10.1 at 0.27 GPa to 12.2 around 0.65 GPa. At higher pressures CN increases only slightly up to 13.1 at 3.75 GPa. Thus, we observe an increase of a CN with relatively low values, indicating a loosely packed gaslike structure, to a close packed more liquidlike structure around 0.65 GPa.

The changes of $S(k)$ and $g(r)$ show a combined modification of the short-range and medium-range order structure. To relate this crossover to the FL, we have calculated the position of the FL from MD simulations using two criteria: disappearance of oscillations of velocity autocorrelation function (VAF) and $c_v = 2k_B$ [17]. VAFs are defined as $Z(t) = \frac{1}{3N}\langle\sum\frac{\mathbf{V}_i(t)\mathbf{V}_i(0)}{\mathbf{V}_i(0)^2}\rangle$, where $\mathbf{V}_i(t)$ is ith particle velocity at time t. The heat capacities were obtained from the fluctuations of kinetic energy in microcanonical ensemble: $\langle K^2\rangle - \langle K\rangle^2 = \frac{3k_B^2T^2}{2N}(1-\frac{3k_B}{2c_V})$, where K is the kinetic energy of the system [34]. We show the examples of VAF and c_v in Fig. 4. The two criteria result in almost perfectly coinciding FL curves in Fig. 5.

From the calculations according to the two criteria above, we find that at room temperature the FL is at 0.65 ± 0.02 GPa, the same pressure where we have observed the structural crossover in our experiments.

Our data enable us to estimate the width of the crossover at the FL. The height and position of the first peak of $S(k)$ (see Fig. 2) as well as the maximum of the third peak undergo a crossover in the range 0.65–0.99 GPa, half-width of which, 0.17 GPa, is usually taken as the maximal width of the crossover. This gives the pressure at the FL crossover as $P_F = 0.65 \pm 0.08$ GPa. Using the slope of the calculated

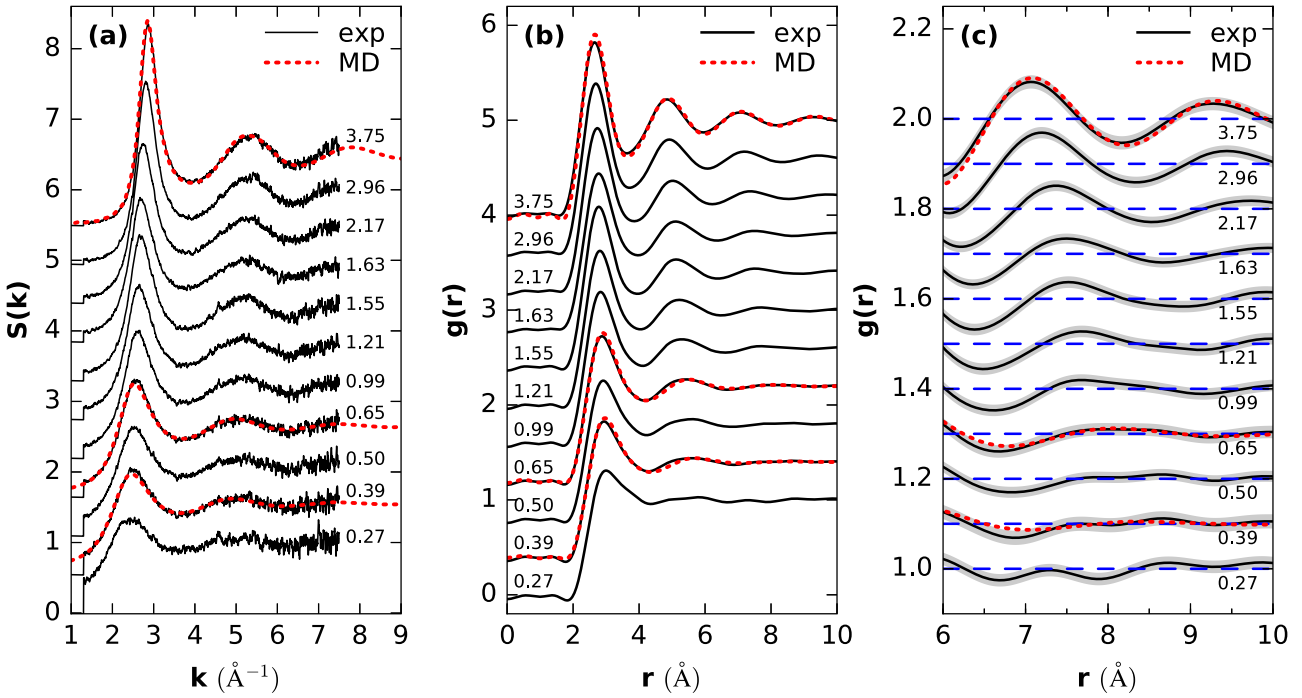

FIG. 1. (a) Structure factors $S(k)$ of neon at different pressures. (b) Radial distribution functions $g(r)$ of neon obtained by Fourier transform of the structure factors. (c) Detail view of $g(r)$ at large distances. The pressures are given next to the curves. The black solid and red dashed curves represent experimental (exp) and molecular dynamics (MD) data, respectively. The shaded area in (c) indicates the error, which was calculated by using the standard deviation of $g(r)$ below the first peak; the dashed straight blue line is showing a value of 1 for each $g(r)$ as a guide for the eye. MD radial distribution functions have been calculated with the same cutoff in $S(k)$ as the experimental data and also using a Lorch modification function in order to get comparable results.

FL (see below), this gives the crossover temperature $T_F = 300 \pm 30$ K. Therefore, the relative width of the FL crossover in pressure and temperature is smaller than 10–12%.

The microscopic origin of the structural crossover at the FL is related to the qualitative change of particle dynamics. As discussed above, below the FL particles oscillate around quasiequilibrium positions and occasionally jump between them. The average time between jumps is conveniently quantified by liquid relaxation time τ. This implies that a static structure exists during τ for a large number of particles, giving rise to the well-defined medium-range order comparable to that existing in structurally disordered solids.

Therefore, we expect liquid-like structural correlations at distances extending the cage size and beyond, e.g., at

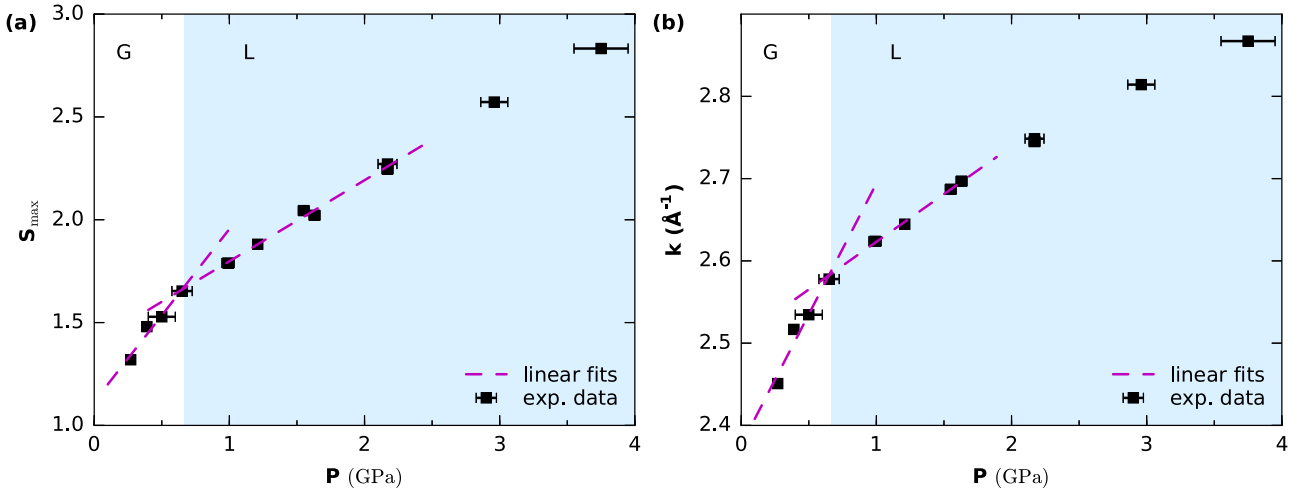

FIG. 2. Extracted height (a) and position (b) of the first maximum of the experimentally derived structure factor $S(k)$ against pressure. The dashed magenta lines show the difference in slopes below and above the crossover. The background shadings indicate the region for gaslike (G) and liquidlike (L) supercritical fluid.

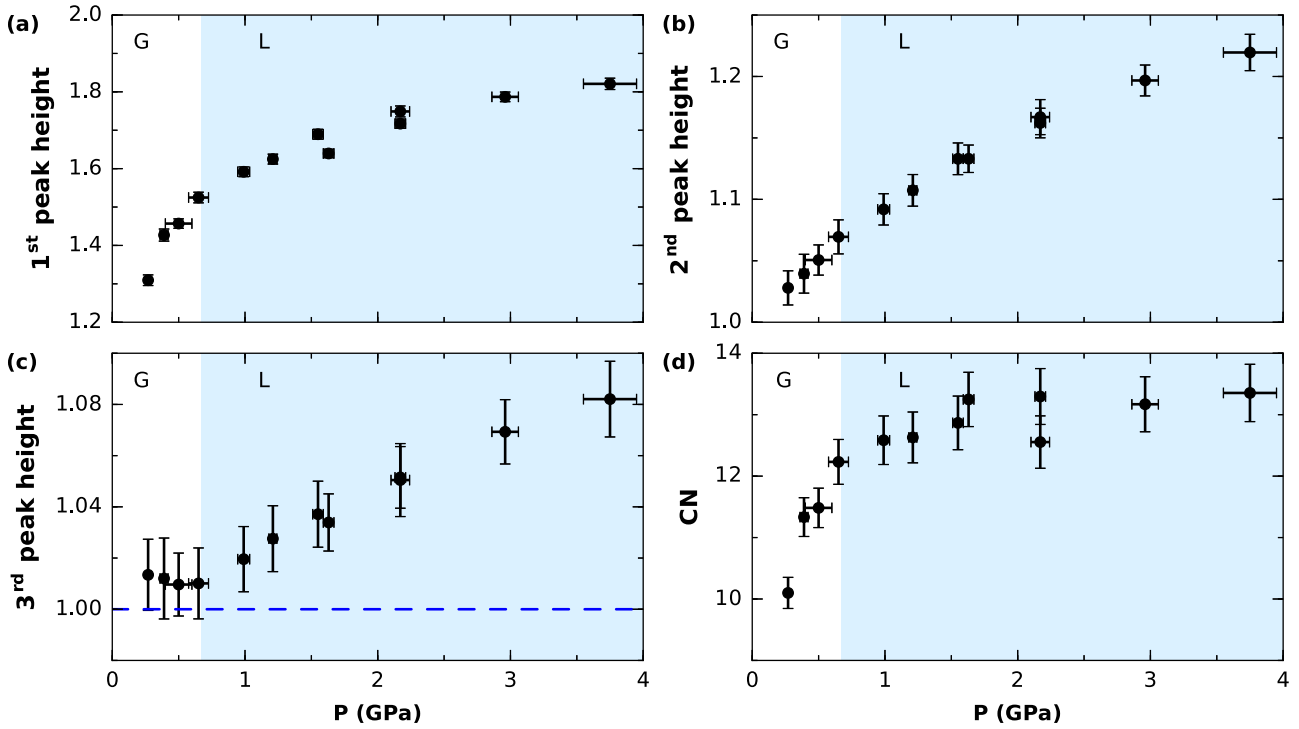

FIG. 3. Maxima of the first (a), second (b), and third (c) peak of the experimentally derived $g(r)$ of neon against pressure. Error bars are calculated from the standard deviation of $g(r)$ below the first peak. Dashed blue vertical line in (c) at 1 serves as a guide for the eye. Coordination number (CN) obtained by integrating $g(r)$ up to the minimum after the first peak is shown in (d). The background shadings indicate the region for gaslike (G) and liquidlike (L) supercritical fluid.

larger distances than 6 Å [see Fig. 1(c)]. Above the FL the particles lose the oscillatory component of motion and start to move in a purely diffusive manner as in gases. A recent study reporting high-resolution MD simulations using Lennard-Jones potentials of different supercritical fluids [36] found differences in the temperature dependence of the $g(r)$ peak heights at the FL. Our experimental data suggests a constant third peak height in the gaslike region indicating loss of medium range order across the FL. However, the error bars of the experimental results are large and the data might not be accurate enough to observe a further decrease in third peak height or slight deviations from the pressure dependence of the first two peaks in $g(r)$. Therefore, a clear answer to whether a loss of medium range order or only a change in the pressure dependence of the peak heights occur at the FL cannot be given based on our current data. The question also arises whether Lennard-Jones potentials can accurately model all interactions of even simple supercritical fluids like neon.

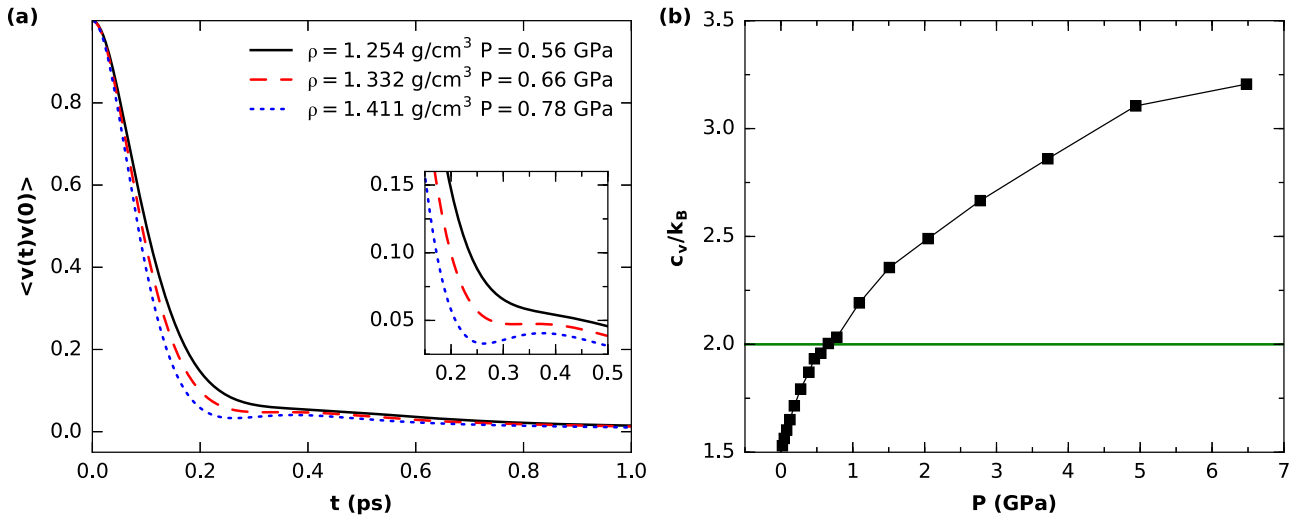

FIG. 4. (a) Velocity autocorrelation functions of Ne derived from MD simulations in the vicinity of the crossover pressure. (b) Isochoric heat capacities of neon derived from MD simulations at $T = 290$ K. The horizontal line marks $c_v = 2k_B$.

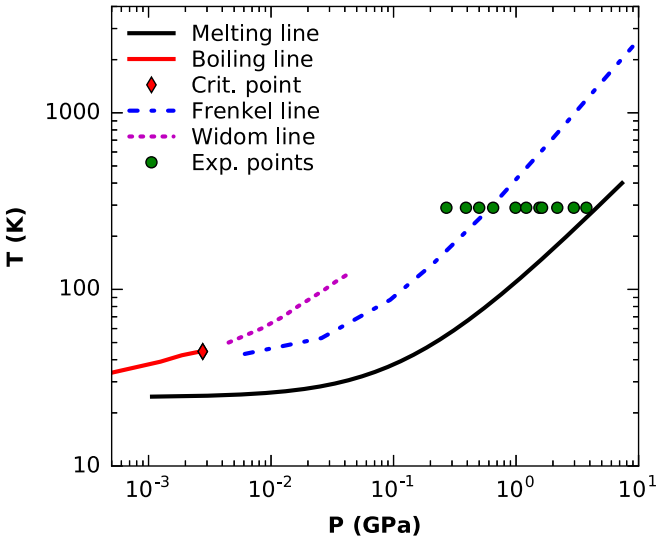

FIG. 5. The calculated Frenkel line for neon, shown together with the boiling line, melting line, Widom line (calculated from maximum of heat capacity taken from Ref. [35]), and experimental points in this study.

While we observe a good agreement between our experimental and simulation data, the agreement is still not absolutely perfect. The interaction might need to be modeled by more sophisticated potentials or even with first-principle methods. A more clear explanation for the change of particle dynamics at the FL comes from the change of CN. The different dynamical regimes are characterized by the change from a close-packed local configuration with 12-fold and above coordination below the FL to a less densely packed system above the FL [see Fig. 3(d)].

Another interesting insight into the origin of the structural crossover comes from the relationship between structure and thermodynamics. The system energy can be written as an integral over the pair distribution function $g(r)$ as

$$E = \frac{3}{2}k_B T + 2\pi\rho \int_0^\infty r^2 U(r) g(r) dr, \qquad (3)$$

where $\rho = N/V$ is number density and $U(r)$ is interatomic potential.

For the case of harmonic modes, phonons, E in (2) can be written as $E = E_0 + E_T$, where E_0 is the energy at zero temperature and E_T is the phonon thermal energy. The collective modes undergo the crossover at the FL and so does the energy. In particular, the transverse modes below the FL start disappearing starting from the lowest frequency equal $\frac{1}{\tau}$ [37] and disappear completely above the FL [18]. Above the FL, the remaining longitudinal mode starts disappearing starting from the highest frequency $\frac{2\pi c}{L}$, where L is the particle mean free path (no oscillations can take place at distance smaller than L) [37]. This gives qualitatively different behavior of the energy below and above the FL, resulting in the crossover at the FL. According to (3), the crossover of energy necessarily implies the crossover of $g(r)$.

We have confirmed this mechanism by calculating the collective modes and their dispersion curves directly. We calculate the longitudinal and transverse current correlation

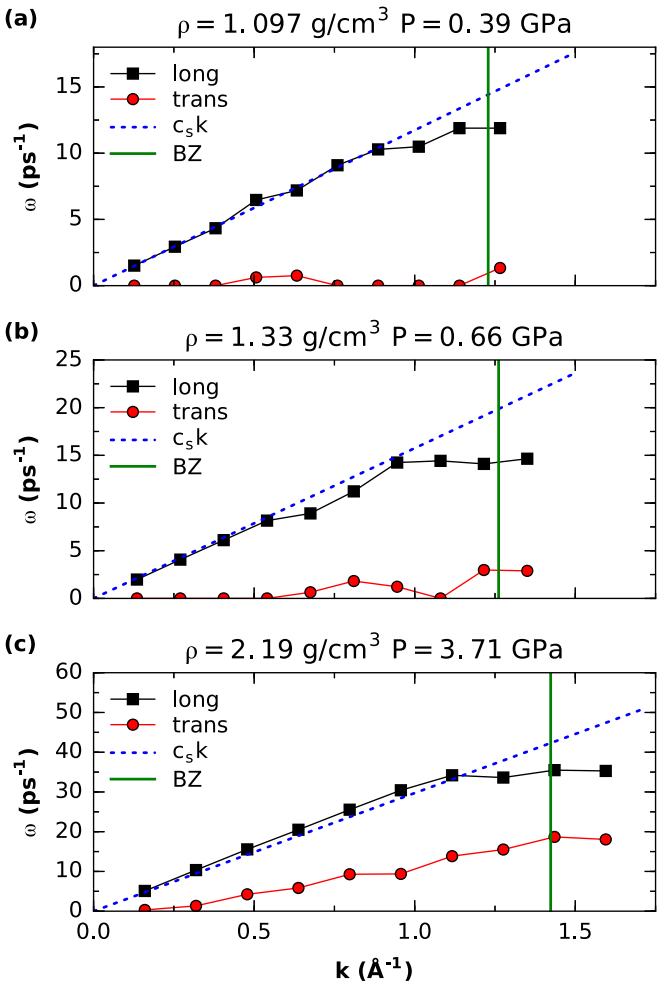

FIG. 6. Excitation spectra of neon derived from MD simulations at pressure points (a) above (b) nearly at and (c) below the Frenkel line. Longitudinal (squares) and transverse (circles) spectra are shown. The dashed lines give the Debye dispersion law $\omega = c_s k$, where c_s is the adiabatic speed of sound. The vertical lines mark the boundary of pseudo-Brillouin zone (BZ).

functions C_L and C_T as

$$C_L(k,t) = \frac{k^2}{N}\langle J_z(\mathbf{k},t)\cdot J_z(-\mathbf{k},0)\rangle$$

$$C_T(k,t) = \frac{k^2}{2N}\langle J_x(\mathbf{k},t)\cdot J_x(-\mathbf{k},0) + J_y(\mathbf{k},t)\cdot J_y(-\mathbf{k},0)\rangle,$$

where $J(\mathbf{k},t) = \sum_{j=1}^{N} \mathbf{v}_j e^{-i\mathbf{k}\mathbf{r}_j(t)}$ is the velocity current [38,39].

The maxima of Fourier transforms $\tilde{C}_L(\mathbf{k},\omega)$ and $\tilde{C}_T(\mathbf{k},\omega)$ give the frequencies of longitudinal and transverse excitations. The resulting dispersion curves are shown in Figs. 6(a)–6(c) at pressures below, nearly at, and above the Frenkel line. We observe that transverse excitations are seen in a large part of the first pseudo-Brillouin zone at high pressure below the FL. At low pressure above the line, the transverse excitations disappear. At the line itself, only small traces of transverse modes close to the boundary can be resolved.

We therefore find that collective excitations undergo a qualitative crossover at the FL, consistent with the earlier

predictions as well as with the structural crossover via Eq. (3). An interesting consequence of the existence of transverse modes below the FL is positive sound dispersion (PSD), the increase of the speed of sound above its adiabatic hydrodynamic value. In Fig. 6 we show the adiabatic speed of sound calculated as $c_s = \gamma^{1/2} c_T$, where $c_T = (\frac{dP}{d\rho})_T^{1/2}$ is the isothermal speed of sound and $\gamma = c_P/c_V$ is the ratio of isobaric and isochoric heat capacities. The isobaric heat capacity was calculated as $c_P = c_V + \frac{T}{\rho^2}(\frac{\partial P}{\partial T})_\rho^2 (\frac{\partial P}{\partial \rho})_T^{-1}$.

We observe the PSD below the FL but not above. This is consistent with the known effect of increase of the longitudinal speed of sound in the presence of shear rigidity (shear waves) over its hydrodynamic value [18,37]. Therefore, the PSD can be discussed on the basis of a visco-elastic model as a result of the presence of transverse modes in the supercritical system. We note that PSD was previously related to the Widom line [9] in view of the change of the dynamic structure factor [1–3]. However, we note that the Widom line exists close to the critical point only and disappears well above the critical point as is the case for conditions discussed in this work [10–13].

Another interesting consequence of our results is the possibility to observe liquid-liquid phase transitions in the supercritical state. So far liquid-liquid transitions involving the change of the medium-range order have been observed below the critical point only [40]. In this work, we have ascertained that the medium range is present in the supercritical state too, as long as the system is below the FL. Therefore, we propose that liquid-liquid phase transitions can be observed above the critical point below the FL.

We propose that our results can be relevant for industrial application of supercritical technologies [41]. Supercritical fluids combine high density (2–3 times higher than the density at the triple point) and high diffusion coefficient that are orders of magnitude higher than those of subcritical liquids. This leads to remarkable increase of solubility and speedup of chemical reactions. Interestingly, the solubility maxima lie very close to the Frenkel line [21] increasing pressure along the FL gives higher density and diffusivity and minimal viscosity. The data of the FL can enhance the supercritical technologies, particularly at higher pressure in the range 1–3 GPa where high-pressure chambers can have large volume.

In summary, we have directly ascertained a structural crossover in the supercritical state. Of particular importance is that the crossover operates at extremely high pressure and temperature: $6.6T_c$ and $250P_c$. The relative width of the crossover is fairly narrow and is less than 10% in both pressure and temperature. Comparing our experimental results with MD simulations enables us to consider the Frenkel line as a boundary between liquidlike and gaslike states of supercritical matter.

ACKNOWLEDGMENTS

We are grateful to G. Simeoni, V. N. Ryzhov, E. N. Tsiok, and J. E. Proctor for fruitful discussions. Yu.D.F. thanks the Russian Scientific Center at Kurchatov Institute and Joint Supercomputing Center of Russian Academy of Science for computational facilities. Yu.D.F. (molecular dynamic simulations, the discussions of the results, writing paper) and V.V.B. (formulation of the problem, the discussions of the results, writing paper) are grateful to Russian Science Foundation (14-22-00093) for the financial support. K.T. is grateful to the Royal Society for support. We thank S. Tkachev for his help during gas loading. Use of the COMPRES-GSECARS gas loading system was supported by COMPRES under NSF Cooperative Agreement EAR 11-57758 and by GSECARS through NSF Grant No. EAR-1128799 and DOE Grant No. DE-FG02-94ER14466. Portions of this work were performed at GeoSoilEnviroCARS The University of Chicago, Sector 13), Advanced Photon Source (APS), Argonne National Laboratory. GeoSoilEnviroCARS is supported by the National Science Foundation-Earth Sciences (EAR-1128799) and Department of Energy-GeoSciences (DE-FG02-94ER14466). This research used resources of the Advanced Photon Source, a U.S. Department of Energy (DOE) Office of Science User Facility operated for the DOE Office of Science by Argonne National Laboratory under Contract No. DE-AC02-06CH11357.

[1] F. Bencivenga, A. Cunsolo, M. Krisch, G. Monaco, G. Ruocco, and F. Sette, Europhys. Lett. **75**, 70 (2006).
[2] F. Gorelli, M. Santoro, T. Scopigno, M. Krisch, and G. Ruocco, Phys. Rev. Lett. **97**, 245702 (2006).
[3] G. G. Simeoni, T. Bryk, F. A. Gorelli, M. Krisch, G. Ruocco, M. Santoro, and T. Scopigno, Nat. Phys. **6**, 503 (2010).
[4] M. E. Fisher and B. Widom, J. Chem. Phys. **50**, 3756 (1969).
[5] C. Vega, L. F. Rull, and S. Lago, Phys. Rev. E **51**, 3146 (1995).
[6] M. Smiechowski, C. Schran, H. Forbert, and D. Marx, Phys. Rev. Lett. **116**, 027801 (2016).
[7] M. Bernabei, A. Botti, F. Bruni, M. A. Ricci, and A. K. Soper, Phys. Rev. E **78**, 021505 (2008).
[8] M. Bernabei and M. A. Ricci, J. Phys.: Condens. Matter **20**, 494208 (2008).
[9] L. Xu, P. Kumar, S. V. Buldyrev, S.-H. Chen, P. H. Poole, F. Sciortino, and H. E. Stanley, Proc. Natl. Acad. Sci. USA **102**, 16558 (2005).
[10] V. V. Brazhkin, Y. D. Fomin, A. G. Lyapin, V. N. Ryzhov, and E. N. Tsiok, J. Phys. Chem. B **115**, 14112 (2011).
[11] V. V. Brazhkin and V. N. Ryzhov, J. Chem. Phys. **135**, 084503 (2011).
[12] Y. D. Fomin, V. N. Ryzhov, E. N. Tsiok, and V. V. Brazhkin, Phys. Rev. E **91**, 022111 (2015).
[13] V. V. Brazhkin, Y. D. Fomin, V. N. Ryzhov, E. E. Tareyeva, and E. N. Tsiok, Phys. Rev. E **89**, 042136 (2014).
[14] V. V. Brazhkin, A. G. Lyapin, V. N. Ryzhov, K. Trachenko, Y. D. Fomin, and E. N. Tsiok, Phys. Usp. **55**, 1061 (2012).
[15] V. V. Brazhkin, Y. D. Fomin, A. G. Lyapin, V. N. Ryzhov, and K. Trachenko, JETP Lett. **95**, 164 (2012).

[16] V. V. Brazhkin, Y. D. Fomin, A. G. Lyapin, V. N. Ryzhov, and K. Trachenko, Phys. Rev. E **85**, 031203 (2012).
[17] V. V. Brazhkin, Y. D. Fomin, A. G. Lyapin, V. N. Ryzhov, E. N. Tsiok, and K. Trachenko, Phys. Rev. Lett. **111**, 145901 (2013).
[18] Y. D. Fomin, V. N. Ryzhov, E. N. Tsiok, V. V. Brazhkin, and K. Trachenko, J. Phys.: Condens. Matter **28**, 43LT01 (2016).
[19] Y. D. Fomin, V. N. Ryzhov, E. N. Tsiok, and V. V. Brazhkin, Sci. Rep. **5**, 14234 (2015).
[20] Y. D. Fomin, V. N. Ryzhov, E. N. Tsiok, V. V. Brazhkin, and K. Trachenko, Sci. Rep. **4**, 7194 (2014).
[21] C. Yang, V. V. Brazhkin, M. T. Dove, and K. Trachenko, Phys. Rev. E **91**, 012112 (2015).
[22] D. Bolmatov, V. V. Brazhkin, Y. D. Fomin, V. N. Ryzhov, and K. Trachenko, J. Chem. Phys. **139**, 234501 (2013).
[23] A. K. Soper, Chem. Phys. **258**, 121 (2000).
[24] M. Santoro and F. A. Gorelli, Phys. Rev. B **77**, 212103 (2008).
[25] D. Bolmatov, M. Zhernenkov, D. Zav, S. N. Tkachev, A. Cunsolo, and Y. Q. Cai, Sci. Rep. **5**, 15850 (2015).
[26] V. V. Brazhkin and J. E. Proctor, arXiv:1608.06883.
[27] M. Rivers, V. Prakapenka, A. Kubo, C. Pullins, C. Holl, and S. Jacobsen, High Press. Res. **28**, 273 (2008).
[28] H. K. Mao, J. Xu, and P. M. Bell, J. Geophys. Res. **91**, 4673 (1986).
[29] G. Weck, G. Garbarino, S. Ninet, D. Spaulding, F. Datchi, P. Loubeyre, and M. Mezouar, Rev. Sci. Instrum. **84**, 063901 (2013).
[30] C. Prescher and V. B. Prakapenka, High Press. Res. **35**, 223 (2015).
[31] J. H. Eggert, G. Weck, P. Loubeyre, and M. Mezouar, Phys. Rev. B **65**, 174105 (2002).
[32] S. K. Oh, J. Thermodyn. (2013) 828620.
[33] S. Plimpton, J. Comput. Phys. **117**, 1 (1995).
[34] D. Frenkel and B. Smit, in *Understanding Molecular Simulation* (Academic Press, London, 2002), p. 638.
[35] E. Lemmon, M. McLinden, and D. G. Friend, in *NIST Chemistry WebBook, NIST Standard Reference Database Number 69*, edited by P. Linstrom and W. Mallard (National Institute of Standards and Technology, Gaithersburg, MD, 2016).
[36] L. Wang, C. Yang, M. T. Dove, Y. D. Fomin, V. V. Brazhkin, and K. Trachenko, Phys. Rev. E **95**, 032116 (2017).
[37] K. Trachenko and V. V. Brazhkin, Rep. Prog. Phys. **79**, 16502 (2016).
[38] J. P. Hansen and I. R. McDonald, in *Theory of Simple Liquids*, 4th ed. (Academic Press, San Diego, 2013), p. 636.
[39] D. C. Rapaport, in *The Art of Molecular Dynamics Simulations* (Cambridge University Press, Cambridge, 1995), p. 564.
[40] V. V. Brazhkin, S. V. Buldyrev, V. N. Ryzhov, and H. E. Stanley (eds.), *New Kinds of Phase Transitions: Transformations in Disordered Substances, Proceeding of NATO Advanced Research Workshop, Volga River* (Kluwer Academic Publishers, Dordrecht, 2002).
[41] E. Kiran, P. Debenedetti, and C. J. Peters, in *Supercritical Fluids* (Springer-Science+Business Media, BV, Dordrecht, 2000), p. 596.